OXIDATION RESISTANCE AND NANOSCALE OXIDATION MECHANISMS IN MODEL BINARY AND TERNARY ALLOYS EXPOSED TO SCW

D.M. Artymowicz[1], C. Andrei[2], J. Huang[2], J. Miles[3], W. Cook[3], G.A. Botton[2] and R.C. Newman[1]

[1] University of Toronto, Ontario, Canada
[2] McMaster University, Hamilton, Ontario, Canada
[3]University of New Brunswick, Fredericton, NB, Canada

Abstract

Model binary and ternary steels were fabricated, containing 9% Cr and 1.5% (atomic) of one of a number of elements (Si, Al, V, Mn, Ti) that might be expected to influence SCW oxidation, using as a general guide the experience with such alloying elements in high-temperature gaseous oxidation. The results reveal a promising effect of alloyed Si on oxidation resistance, although some intergranularity is evident ahead of the oxidation front. Nanoscale, clustered Si enrichment at the uniform oxidation front was revealed by high-resolution analytical electron microscopy of FIB sections, but the details are still under investigation. Internal oxidation of Cr (and/or Si) with various morphologies was also observed near the oxidation front.

1. Introduction

SCW oxidation of alloys is expected to show some of the features of high-temperature gaseous oxidation [1], but takes place in a temperature range where there is relatively little lattice diffusion of substitutional alloying elements. It is of interest to determine the degree to which concepts familiar in high-temperature oxidation (Wagner's theory…healing layers of SiO_2 or Al_2O_3…internal-to-external oxidation transitions) apply to SCW oxidation. Accordingly, binary and ternary alloys based on FeCr and containing various ternary alloying elements have been prepared and exposed to SCW at 500°C. This builds on an earlier phase of the study in which steels with 14% and 25% Cr were oxidized in the same environment and examined by high-resolution analytical electron microscopy [2]. The main findings of that work were as follows:

- that the use of FIB and analytical TEM has enormous potential in the study of SCW oxidation;
- that the 14Cr steel oxidizes relatively rapidly in SCW, with outer Fe-rich and inner Cr-rich oxide layers;
- that the 25Cr steel has very good oxidation resistance in SCW, but grain boundaries can initiate rapid oxidation, apparently due to the presence of a deleterious second phase. This oxidation propagates locally at a rate similar to that of the 14Cr steel. However, it is not certain that Cr depletion due to a deleterious phase is necessary for the propagation of such oxidation.
- that there are indications of internal oxidation at the oxidation fronts in both alloys.

2. Experimental Procedures

Alloys of composition Fe9Cr and Fe9Cr1.5Si (at.%) were prepared in an arc furnace as 1 cm thick billets and cold rolled to the final thickness of 2 mm with no intermediate annealing. Similar alloys were prepared with V, Al, Mn or Ti as the ternary element and will be discussed in another paper.

Rectangular samples 10x20 mm were cut out from the cold rolled plates and air annealed at 800^{o}C for 15 min. Annealing resulted in fully recrystallized microstructures with an average grain diameter of ~50 µm.

After removal of scale formed during annealing one of the following three surface finishes was applied – abrasion with 800 grit paper, polishing with 1 µm diamond slurry or electropolishing.

Samples were exposed to SCW at 500°C and 25 MPa for a total of 500 h. The exposure was interrupted twice, after 100 h and 250 h, in order to record intermediate mass gain. Further exposure details can be found in [3]. All electron microscopy was done on samples after 500 h exposure.

Cross-sectional and surface imaging, as well as sample preparation for transmission electron microscopy (TEM), were carried out on a Zeiss NVision 40 Focused Ion Beam/Scanning Electron Microscope, using the lift-out technique. The TEM observations were performed on a FEI Titan 80-300 instrument fitted with an energy dispersive X-ray spectrometer (Inca model) for elemental mapping and chemical analysis as well as a high-angle annular dark-field detector.

3. Results and Discussion

3.1 Oxidation Kinetics

A promising reduction in oxidation kinetics was achieved by the addition of 1.5 at% Si to the 9% Cr alloy, as shown in Figure 1. This type of behaviour is typical of a situation where the ternary element forms an oxide at the interface between the alloy and an inner, Cr-rich oxide. Initially the ternary alloy shows a more-or-less parabolic oxidation behaviour, but after a time the weight gain starts to level off.

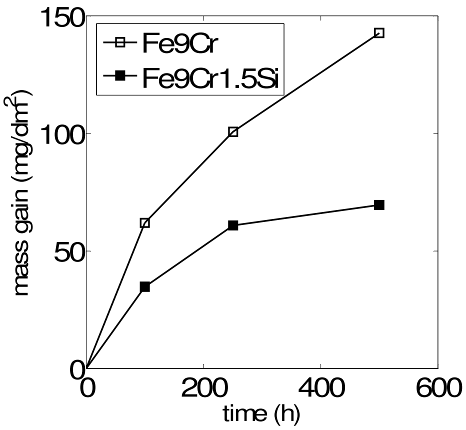

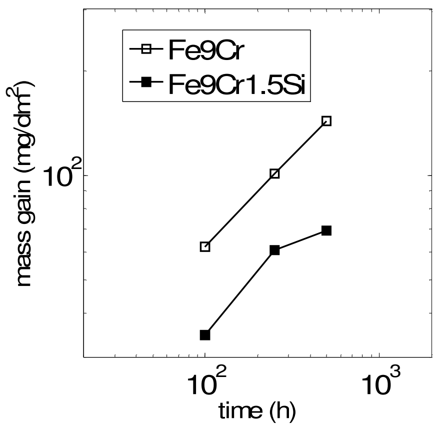

Figure 1 Weight gain curves for the binary and ternary alloys, on linear and log-log scales.

3.2 Microscopy of the Oxidation

As in previous work, there was always an outer, Fe-rich oxide and an inner, Cr-rich oxide, with the boundary between these corresponding approximately to the original alloy surface. Our focus was on the behaviour of Si within this structure.

Figure 2 shows an example of the extraction of a FIB section from an oxidized surface of the binary FeCr alloy with the 800 grit finish surface. The outer, Fe-rich and inner, Cr-rich layers are visible. This sequence of oxides was common for all analyzed samples. The capping layer used to protect the surface during sectioning was carbon.

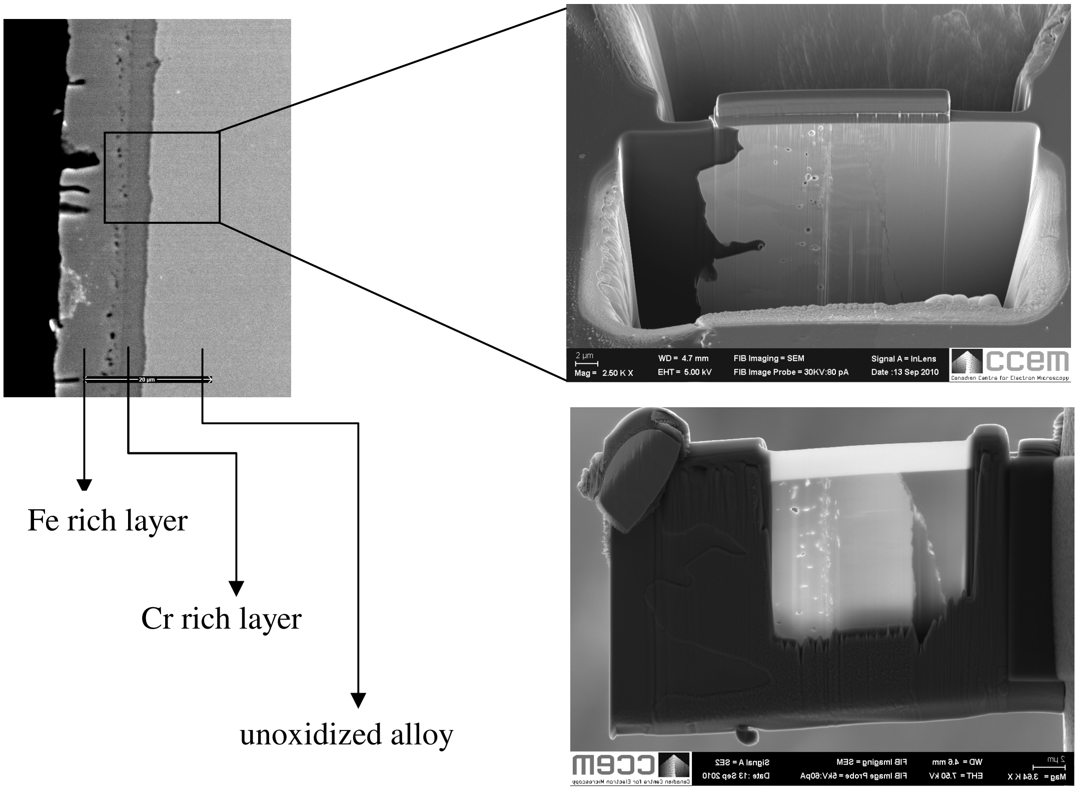

Figure 2 Sequence of steps in the extraction of an electron-transparent FIB section from a SCW-oxidized surface of Fe9Cr with an 800 grit surface finish after 500 h SCW exposure. The image in the lower right corner has been intentionally flipped so that the orientation is the same in all three images.

There was a pronounced tendency for intergranular oxidation in all the alloys, although this was not of any great extent compared with the depth of oxidation on grain surfaces. Figure 3 shows Cr-rich intergranular oxide projecting from the inner, Cr-rich oxide layer on the binary alloy (electropolished surface). Clearly Fe has migrated outwards through both these structures, creating a strong Fe depletion. The Cr X-ray map shows relatively little contrast between the surface oxide and the underlying alloy, but there is a strong contrast with the intergranular Cr enrichment. The reasons for these subtleties are under investigation. Examination of the interface between the Cr-rich oxide and the alloy in transmission at higher magnification did not show any special features such as internal oxidation.

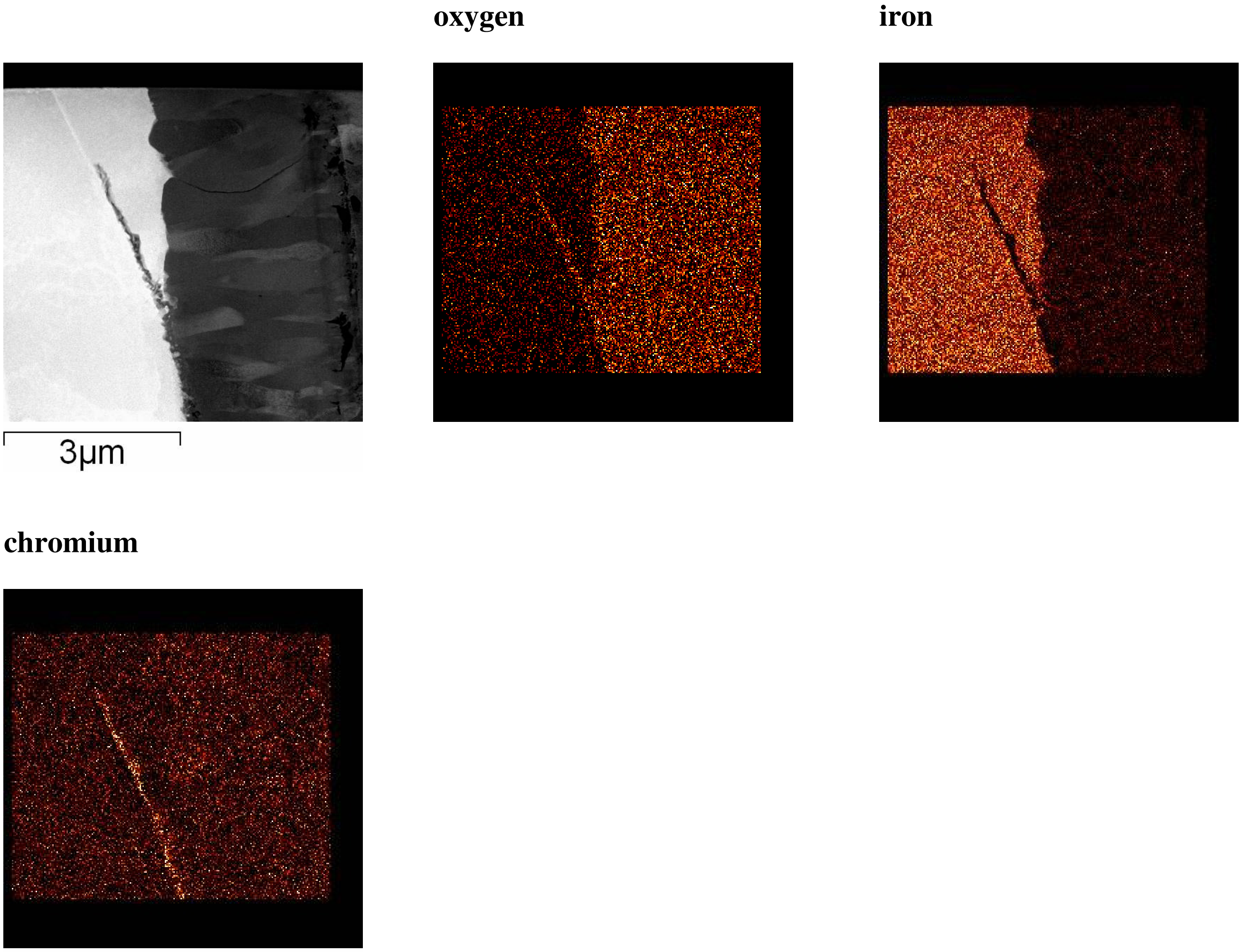

Figure 3 Microscopy and analysis of the inner Cr-rich oxide layer and underlying intergranular oxidation on the binary alloy exposed for 500 h in SCW. Surface finish - electropolishing.

The ternary alloy showed a much more complex behaviour near the interface between the Cr-rich oxide and the alloy. Not surprisingly, its lower overall oxidation kinetics led to a slightly more evident intergranularity, although the maximum depth of intergranular oxidation, measured from the original alloy surface, was similar to that of the binary alloy. The intergranular oxide had a very high Si content - Figure 4 - but it was challenging to create an X-ray map of Si near the general oxide-metal interface. In Figure 5 there is only a hint that Si is clustered together with O and Cr in the filamentous oxidized features near this interface. However spot analyses clearly showed that the suspected Si-rich areas were indeed rich in Si and O as well as Cr – Figure 6.

There is almost certainly oxidized Si within the Cr-rich layer as well as at the interface, as the morphology of the Cr-rich layer is quite different from that on the binary alloy.

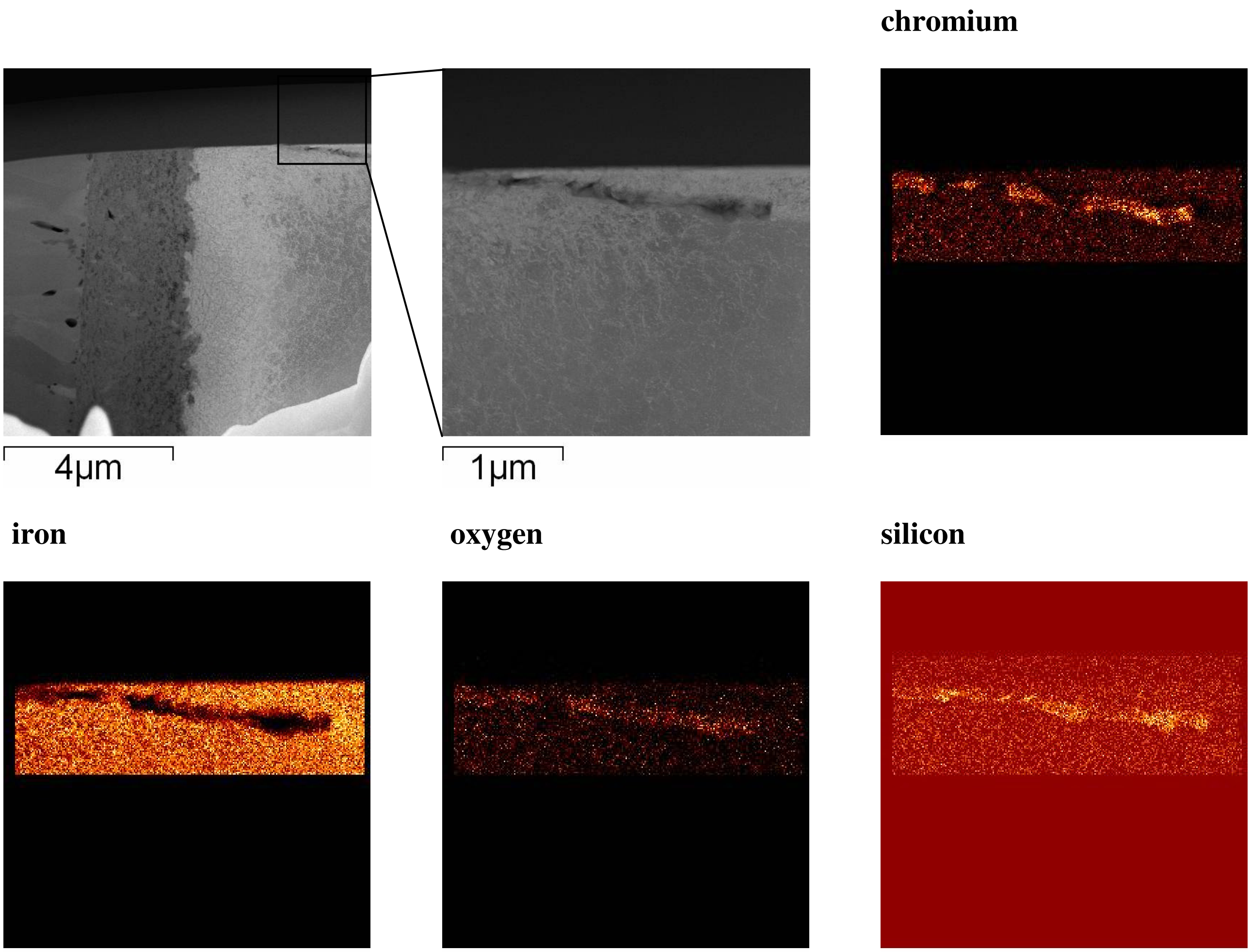

Figure 4 Microscopy and analysis of intergranular oxidation on the ternary alloy. Surface finish - 1μm diamond slurry.

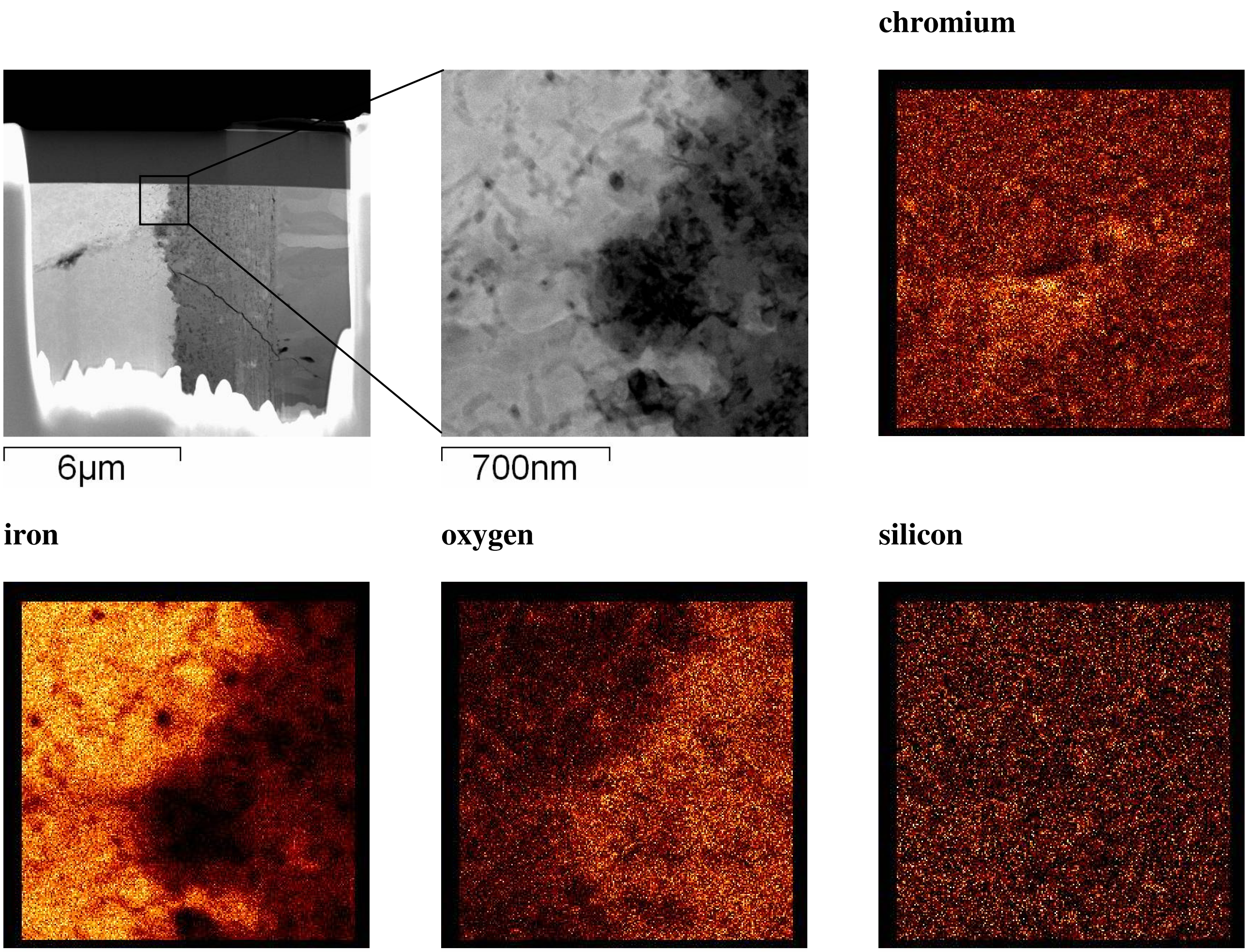

Figure 5 Microscopy and analysis of the main oxide-alloy interface on the ternary alloy. Surface finish – 800 grit paper.

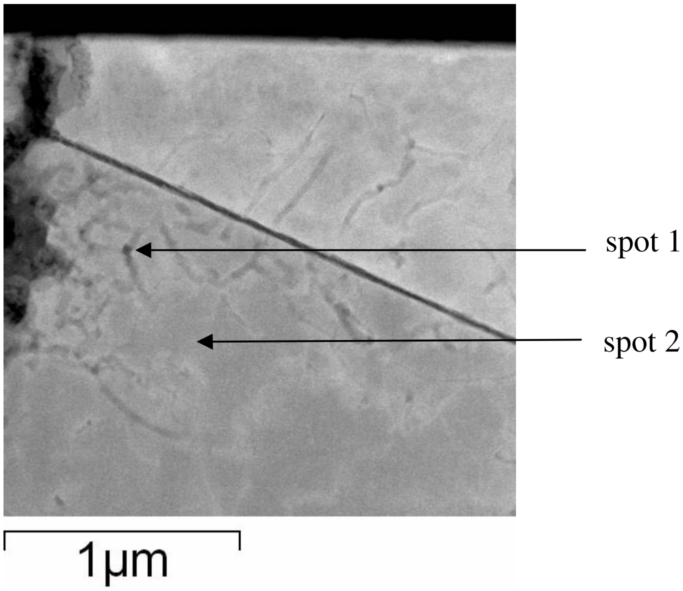

	spot 1	spot 2
C	14.37	10.26
O	32.01	3.64
Si	4.09	1.23
Cr	17.36	8.03
Fe	32.17	76.82

Figure 6 Spot analysis of oxide filaments near the oxide-alloy interface on the ternary alloy, showing Si and O enrichment. Composition in atomic percent. Surface finish – electropolishing.

As an interim conclusion, we can say that Si does accumulate near the interface between the Cr-rich oxide and the alloy, but it is not certain that this is the rate-determining process in the oxidation, as there is also an effect within the Cr-rich oxide itself.

Preliminary results showed that in both alloys the deformation zones created by 1 µm diamond slurry and 800 grit paper were much shallower than the progress of the oxidation front and thus affected only the early stages of oxidation. Detailed analysis will be presented elsewhere together with the influence on oxidation of small additions of Al, Mn, Ti and V [4].

4. Conclusions

1. Binary FeCr and ternary FeCrSi alloys show fairly analogous behaviour in SCW oxidation as in ordinary steam oxidation, but with many subtleties.

2. Si does give additional protection, via its enrichment near the general oxide-alloy interface and probably also in the inner Cr-rich oxide itself.

3. There is pronounced intergranularity to the oxidation, which is more evident in the ternary alloy.

5. References

[1] S.R.J. Saunders, M. Monteiro and F. Rizzo, "The Oxidation Behaviour of Metals and Alloys at High Temperatures in Atmospheres Containing Water Vapour : A Review", *Progress in Materials Science*, 53, 775-837 (2008).

[2] D.M. Artymowicz, C. Andrei, J. Huang, J. Miles, W. Cook, G.A. Botton and R.C. Newman, "Preliminary Study of Oxidation Mechanisms of High Cr Steels in Supercritical Water", Proc. Canada-China Joint Workshop on Supercritical Water-Cooled Reactors, Toronto, 2009 (proceedings on CD).

[3] Orfino, F., Yao, B. Xie, Y., Yick, S., Miles, J. Cook, W. and Hui, R.,"Ceramic Coatings for Metallic Components in Supercritical Water-CooledReactors", these proceedings.

[4] D.M. Artymowicz, C. Andrei, J. Huang, J. Miles, W. Cook, G.A. Botton and R.C. Newman, "Influence of Cold Work On Oxidation Mechanisms of Fe based Binary and Ternary Alloys in Supercritical Water" – in preparation.

6. Acknowledgements

This research was funded by NRCan, NSERC and AECL under the Generation IV Energy Technologies program. Discussions with David Guzonas and Wenyue Zheng are gratefully acknowledged. Alloys used in this work were provided by Materials Preparation Center of the Ames Laboratory, Ames, Iowa. The electron microscopy work was carried out at the Canadian Centre for Electron Microscopy, a facility supported by McMaster University and NSERC.